Journal of Statistical Physics, Vol. 44, Nos. 3/4, 1986

The Fast Rate Limit of Driven Diffusive Systems

J. Krug,[1] J. L. Lebowitz,[2] H. Spohn,[1] and M. Q. Zhang[2]

Received January 13, 1986

We study the stationary nonequilibrium states of the van Beijeren/Schulman model of a driven lattice gas in two dimensions. In this model, jumps are much faster in the direction of the driving force than orthogonal to it. Van Kampen's Ω-expansion provides a suitable description of the model in the high-temperature region and specifies the critical temperature and the spinodal curve. We find the rate dependence of T_c and show that independently of the jump rates the critical exponents of the transition are classical, except for anomalous energy fluctuations. We then study the stationary solution of the deterministic equations (zeroth-order Ω-expansion). They can be obtained as trajectories of a dissipative dynamical system with a three-dimensional phase space. Within a certain temperature range below T_c, these equations have a kink solution whose asymptotic densities we identify with those of phase coexistence. They appear to coincide with the results of the "Maxwell construction." This provides a dynamical justification for the use of this construction in this nonequilibrium model. The relation of the Freidlin–Wentzell theory of small random perturbations of dynamical systems to the steady-state distribution below T_c is discussed.

KEY WORDS: Stationary nonequilibrium states; driven lattice gas; van Kampen's Ω-expansion; "Maxwell construction."

1. INTRODUCTION

Stochastic lattice gases are widely studied kinetic models for a variety of physical phenomena. In their simplest particle-conserving version (Kawasaki dynamics in spin language), particles jump on a lattice respecting single site occupancy. Their jump rates satisfy detailed balance with respect to some energy, H. Therefore the stationary states for a fixed number of particles have the equilibrium form $Z^{-1}\exp[-\beta H]$. For an

[1] Theoretische Physik, Theresienstr. 37, 8 Munchen 2, FRG.
[2] Department of Physics and Mathematics, Rutgers University, New Brunswick, New Jersey 08903.

0022-4715/86/0800-0535$05.00/0

attractive interaction the system segregates into a low- and a high-density phase at sufficiently low temperature.

In Refs. 1 and 2 two of us posed the problem of how the statistical properties of the lattice gas are altered when jump rates are chosen in such a way that the stationary state(s) is no longer an equilibrium state for any (known) H. In particular, we considered jumps biased in a certain direction. Physically the bias may be thought to originate from an external driving force, $\mathbf{E}$. For example, we may imagine that the particles are charged and that a uniform external electric field acts upon the system. Our motivation was threefold: First, we wanted to understand how the driving force alters, if at all, the segregation transition, similar in spirit to the investigation of Kawasaki and Onuki[3,4] of a binary fluid under shear. Second, a driven stochastic lattice gas seemed to be the simplest model, with spatial structure, which could give general properties of noneqilibrium steady states. Finally, this system is thought to model some fast ionic conductors.[5]

To answer these questions we studied the driven lattice gas by means of a Monte Carlo simulation.[1,2] The essential observations were:

— the segregation transition persists at any field strength

— the ordered phase is highly anisotropic with striplike tyical configurations in the field direction

— the critical temperature is shifted upwards as $\mathbf{E}$ increases; the critical exponents appear to be changed compared to $\mathbf{E}=0$

— the average current has a break in its slope at the critical temperature.

These results were corroborated by more extensive runs.[6–8] In particular, in two dimensions the critical exponent β, corresponding to the difference in density of the two phases, appears to be around 0.3: this is to be compared with the Onsager result 0.125 and the mean field value 0.5.

To obtain an understanding of this system, van Beijeren and Schulman[9] consider a modified version of the driven lattice gas, where the jumps in the field direction are very fast compared to the jumps orthogonal to it and the driving field is infinite, i.e., no jumps opposite to the field. In this fast-rate limit the spatial dimension of the model reduces by one. Furthermore, fluctuations in the system are small, of the order $1/N$, where N is the column height (the fast exchange direction). Therefore the model comes in reach of an analytical study. The goal of this paper is a detailed and systematic investigation of the van Beijeren/Schulman (vBS) model.

Three aspects, not discussed in Ref. 9, are our main interest:

(i) In a Monte Carlo simulation one usually employs the Metropolis

rates as giving the largest exchange rate per time step. If the goal is the simulation of typical equilibrium configurations, then the choice of jump (or flip) rates is of no importance, as long as detailed balance is satisfied. In the present case, however, the steady-state distribution depends, in general, on the specific jump rates, since it is *only* defined as the stationary solution of a certain master equation. One hopes that certain features, e.g., the topology of the phase diagram and critical exponents, are independent of the specific rates. A check on this is provided by investigating the rate dependence in the vBS model.

(ii) vBS use the Maxwell construction ($\equiv$ equality of the "chemical potential" of the two phases) in order to determine the phase coexistence curve. *A priori*, it is not clear that this concept, familiar from equilibrium statistical mechanics, can also be applied to the present nonequilibrium situation. In fact, there is no obvious *a priori* way for defining the chemical potential. We give a dynamical method for finding the coexisting phases by requiring the existence of a stable kink profile with asymptotic densities lying on the phase coexistence curve. This is constructed numerically for the rates used by vBS and appears to agree (near the critical point at least) with the results obtained via the Maxwell construction.

(iii) The low-temperature dynamics is complicated, as already hinted at in Ref. 9. We study it by means of the Freidlin–Wentzell theory of small random perturbations of dynamical systems. A crucial role is played by the stationary solutions of the limiting, $N \to \infty$, deterministic dynamics. They can be regarded as the trajectories of a discrete dynamical system with a three-dimensional phase space. This is analogous to some mean-field equilibrium models.[17–21] The fixed point structure and the periodic orbits of this discrete dynamical system provide a certain insight into the low-temperature dynamics.

1.1. Field Theoretic Formulation

Before going on to discuss the above topics, we note that close to the critical point one may hope to describe the essential properties of the driven lattice gas by a time-dependent Ginzburg–Landau theory.[10] Since the order parameter is conserved, the Cahn–Hilliard equation, alias model B, is appropriate. If $\phi(x, t)$ denotes the local order parameter of the system, then the equations of motion for the system without driving force are[10]

$$\frac{\partial}{\partial t}\phi + \operatorname{div} \mathbf{j} = 0 \tag{1.1}$$

$$\mathbf{j} = -L \operatorname{grad} \frac{\delta H}{\delta \phi} + L^{1/2}\mathbf{j}_{\text{ran}} \tag{1.2}$$

Here H is the Ginzburg–Landau–Wilson free energy functional in the standard form,

$$H[\phi] = \beta \int d^d x \{\tfrac{1}{2}|\text{grad}\, \phi(x)|^2 + V(\phi(x))\} \tag{1.3}$$

with $V(\phi) = \frac{1}{2}r\phi^2 + g\phi^4$, $g > 0$. Equation (1.1) expresses the local conservation law. The right-hand side of (1.2) splits the density current $\mathbf{j}$ into two parts: a systematic part proportional to the gradient of the chemical potential and a random part which models the fast microscopic processes. The latter is Gaussian and δ-correlated in space-time. L is the Onsager coefficient which in principle may depend on ϕ, $L > 0$. The stationary solutions to (1.1) and (1.2) are the Gibbs measures $\sim \exp[-\beta H(\phi) + h \int d^d x\, \phi(x)]$ in which the average current vanishes. The driving field is taken into account by adding to (1.2) the term $\sigma \mathbf{E}$, where σ is the conductivity, in general $\mathbf{E}$ and ϕ dependent. Then (1.2) becomes

$$\mathbf{j} = -L\, \text{grad} \frac{\delta H}{\delta \phi} + \sigma \mathbf{E} + L^{1/2} \mathbf{j}_{\text{ran}} \tag{1.4}$$

The stationary solutions of (1.1) together with (1.4) are now no longer known—except for trivial cases.

The critical behavior of the model defined by (1.1) and (1.4) are studied by means of dynamical renormalization. Exploiting supersymmetry, Gawedski and Kupiainen[11] find an upper critical dimension 5 for $L = \text{const}$ and $\sigma = \phi^2$. Leung and Cardy[12] determine the scaling form of the two-point function and compute critical exponents in ε-expansion. An important insight is that the ϕ^4-term is irrelevant in the sense of renormalization group for $\mathbf{E} \neq 0$. Also, since after the first renormalization step the model becomes anisotropic, this should be incorporated from the beginning in (1.3) and (1.4).[13]

Recently the high-temperature behavior of (1.1) and (1.4) for $L = \text{const}$, $\sigma = \phi^2$ has been analyzed[13,14] (cf. also Ref. 15). For dimension $d = 1, 2$ the driving force destroys the usual diffusive steady-state fluctuations. Surprisingly, for $d = 1$ there is a mapping to a SOS model for an interface with quenched random impurities defined by

$$\int \prod_t dx(t) \exp\left[-\int dt \{\dot{x}(t)^2 + V(x(t), t)\} \right] \tag{1.5}$$

where $x(t)$ is the position of the interface relative to a reference line and $V(x, t)$ is white noise in both arguments.[16]

The rest of the paper is organized as follows: In Sec. 2 we recall the lattice gas model of Ref. 2 and its fast-rate limit yielding the vBS

approximation. To this model we apply the Ω-expansion of van Kampen. In Sec. 3 we determine the critical point, critical exponents, and the spinodal for general rates. In Sec. 4 we describe a fairly well understood mean-field equilibrium model which we regard as prototypical for the vBS model, although the latter does not satisfy detailed balance, and we determine the phase coexistence curve. Section 5 deals with the low-temperature dynamics.

2. THE LATTICE GAS MODEL AND ITS Ω-EXPANSION

We consider a lattice gas on a square lattice Λ consisting of N rows and M columns, $MN = |\Lambda|$. The driving field will be oriented vertically. In this direction periodic boundary conditions are imposed. At each lattice site $x \in \Lambda$ there is an occupation variable η_x with values 0, if the lattice site x is empty, 1 if it is occupied. A configuration $\{\eta_x | x \in \Lambda\}$ of particles is denoted by η. The energy of a configuration η is given by the usual nearest-neighbor Ising Hamiltonian

$$H(\eta) = -4J_h \sum_{\substack{|x_1 - y_1| = 1 \\ x_2 = y_2}} \eta_x \eta_y - 4J_v \sum_{\substack{|x_2 - y_2| = 1 \\ x_1 = y_1}} \eta_x \eta_y \tag{2.1}$$

$J_h(J_v)$ is the coupling for horizontal (vertical) bonds.

The dynamics of the model are defined by specifying the rate for the jump of a particle to a neighboring empty lattice site. The driving field favors jumps in the field direction and suppresses jumps opposite to it. Jumps orthogonal to the field are unaffected and satisfy the usual detailed balance condition. We denote by $c_E(x, y, \eta)$ the exchange rate for the occupations at sites x and y when the configuration is η. E indicates the strength of the driving field ($\equiv$ bias). Physically it is rather natural to impose *local detailed balance* [2] in the form

$$c_E(x, y, \eta) = c_E(x, y, \eta^{xy}) \exp[-\beta(H(\eta^{xy}) - H(\eta)) + \mathbf{E} \cdot (x - y)(\eta_x - \eta_y)] \tag{2.2}$$

Here β is the inverse temperature and η^{xy} denotes the configuration η with occupations at x and y interchanged. In the exponent the work done by the driving force during the jump is added to the energy difference for the jump and β is absorbed in E. To put it differently: *locally* the driving force behaves as (minus) the gradient of a linear potential.

The master equation describing the time evolution of the probability distribution $p_t(\eta)$ on configuration space has the form

$$\frac{d}{dt} p_t(\eta) = \sum_{|x-y|=1} [c_E(x, y, \eta^{xy})\, p_t(\eta^{xy}) - c_E(x, y, \eta)\, p_t(\eta)]$$
$$\equiv L_E p_t(\eta) \tag{2.3}$$

For $E=0$ the stationary solutions of (2.3) are the equilibrium distributions at a given average density ρ; $\rho \sim \exp[-\beta H(\eta)]\, \delta(\sum_x \eta_x - NM\rho)$. Also for $E \neq 0$, if the system had "rigid walls" perpendicular to **E**, then the stationary solution is $\exp[-\beta H(\eta) + \sum_x (\mathbf{E} \cdot x)\, \eta_x]\, \delta(\sum_x \eta_x - NM\rho)$. This is, however, not the case if we have periodic boundary conditions in the direction of **E**. The stationary solution of (2.3) now carries a current and does not satisfy detailed balance. In fact, the stationary distribution is unknown, and this is in fact the major difficulty in our problem.

The basic idea of vBS is to postulate jumps in the field direction to be much more frequent than in the direction orthogonal to it and to exploit the resulting separation of time scales. We follow them by setting

$$c_E(x, y, \eta)$$
$$= \begin{cases} \Gamma_{\|} \phi_{\|}(\beta(H(\eta^{xy}) - H(\eta))) - E(x_2 - y_2)(\eta_x - \eta_y)), & x - y = \pm e_2 \\ \Gamma_{\perp} \phi_{\perp}(\beta(H(\eta^{xy}) - H(\eta))), & x - y = \pm e_1 \end{cases} \tag{2.4}$$

and $c_E(x, y, \eta) = 0$ otherwise, where $e_1 (e_2)$ is the unit vector along the horizontal (vertical) direction and $\Gamma_{\perp} (\Gamma_{\|})$ sets the time scale for horizontal (vertical) jumps. By (2.2) the functions $\phi_{\|}$ and $\phi_{\perp}$ have to satisfy

$$\phi(\lambda) = e^{-\lambda} \phi(-\lambda) \tag{2.5}$$

In Ref. 2 Metropolis rates are used corresponding to $\Gamma_{\|} = \Gamma_{\perp}$, $\phi_{\|} = \phi_{\perp} = \phi$, and $\phi(\lambda) = 1$ for $\lambda < 0$, $\phi(\lambda) = e^{-\lambda}$ for $\lambda \geqslant 0$. In Ref. 7 Metropolis rates are used with the ratio $\Gamma_{\|}/\Gamma_{\perp}$ varying between 1 and 80.

In order to separate the time scales, we keep $\Gamma_{\perp}$ fixed, say $\Gamma_{\perp} = 1$, and let $\Gamma_{\|} \to \infty$. For every horizontal jump there are then many jumps in the field direction and therefore between any two horizontal jumps the system equilibrates in a steady state of (2.3) with $\Gamma_{\perp} = 0$. Let n_j be the number of particles in the jth column, $j = 1, ..., M$, $n_j = 0, 1, ..., N$ and $\mathbf{n} = (n_1, ..., n_M)$. Since for $\Gamma_{\perp} = 0$ horizontal jumps are forbidden, for each fixed vector $\mathbf{n}$ there is a unique steady-state solution to (2.3) satisfying

$$L_E w_{\mathbf{n}}(\eta) = 0, \qquad \Gamma_{\perp} = 0 \tag{2.6}$$

On the slow time scale (2.3) reduces as $\Gamma_{\|} \to \infty$ to a "coarse grained" master equation governing the distribution of $\mathbf{n}$,

$$\frac{d}{dt} p_t(\mathbf{n}) = \sum_{\mathbf{n}'} [c^{(N)}(\mathbf{n}', \mathbf{n})\, p_t(\mathbf{n}') - c^{(N)}(\mathbf{n}, \mathbf{n}')\, p_t(\mathbf{n})] \tag{2.7}$$

where the jump rates are defined as

$$c^{(N)}(\mathbf{n}', \mathbf{n}) = N < \phi_\perp(\beta(H(\eta^{xy}) - H(\eta))) > (\mathbf{n}) \tag{2.8}$$

with $\langle \cdot \rangle(\mathbf{n})$ denoting the average with respect to $w_{\mathbf{n}}(\eta)$.

Unfortunately, $\langle \cdot \rangle(\mathbf{n})$ is known explicitly only for particular rates. Following vBS we assume that any jump opposite to $\mathbf{E}$ is forbidden and a jump in the direction of $\mathbf{E}$ is performed provided the hard core exclusion is not violated, i.e.,

$$c_\infty(x, y, \eta) = \begin{cases} \Gamma_\parallel \eta_x(1-\eta_y), & x - y = \pm e_2 \\ \phi_\perp(\beta(H(\eta^{xy}) - H(\eta))), & x - y = \pm e_1 \end{cases} \tag{2.9}$$

and $c_\infty(x, y, \eta) = 0$ otherwise. Then $\langle \cdot \rangle(\mathbf{n})$ is given simply by randomly distributing the particles in each column. Notice that this is equivalent to putting $\phi_\parallel = \text{const}$, i.e., exchanges in the vertical direction behave as if the system was at an infinite temperature. The effect of the strong field is to wash out all correlations within each column. This renders $c^{(N)}(\mathbf{n}', \mathbf{n})$ in (2.8) explicitly computable and so defines the vBS model for general jump rates; vBS set $\phi_\perp(\lambda) = \exp[-\lambda/2]$ for computatinal convenience.

The goal of our paper is to analyze the steady-state distribution of the master equation (2.7) for a large system, $M, N \to \infty$. Since, except for special cases, (2.7) does not satisfy detailed balance, we have to rely on approximate methods. As a crucial simplification we note that for $N \to \infty$ fluctuations are suppressed. Therefore we consider the limit $N \to \infty$ for fixed M.

For large N the natural variables are n_j/N. The rates (2.8) imply then that tyically these densities have N changes of size $1/N$ during a unit time interval. This is precisely the setup of the Ω-expansion[20,21] with the column height N playing the role of the system size parameter Ω. We set

$$\frac{1}{N} n_j(t) = \rho_j^{(N)}(t) + N^{-1/2} \xi_j^{(N)}(t) \tag{2.10}$$

$\rho_j^{(N)}(t)$ is the average density of the jth column at time t, $0 \leqslant \rho_j^{(N)}(t) \leqslant 1$, and $N^{-1/2}\xi_j^{(N)}(t)$ are small fluctuations around the average density. Then in the limit $N \to \infty$, $\rho_j^{(N)}(t) \to \rho_j(t)$ and the local densities are governed by conservation type deterministic equations

$$\frac{d}{dt} \rho_j(t) + J_j(\boldsymbol{\rho}(t)) - J_{j-1}(\boldsymbol{\rho}(t)) = 0 \tag{2.11}$$

The current, $J_j(\boldsymbol{\rho})$, between columns j and $j+1$ is given as the number of jumps (per unit time) from j to $j+1$ minus those from $j+1$ to j,

$$J_j(\boldsymbol{\rho}) = R(\rho_{j-1}, \rho_j, \rho_{j+1}, \rho_{j+2}) - R(\rho_{j+2}, \rho_{j+1}, \rho_j, \rho_{j-1}) \tag{2.12}$$

Here

$$R(\rho_{j-1}, \rho_j, \rho_{j+1}, \rho_{j+2}) = \lim_{N\to\infty} \langle \phi_\perp(\beta(H(\eta^{xy}) - H(\eta))) \rangle (\mathbf{n}) \quad (2.13)$$

with $x_2 = y_2$, $x_1 = j$, $y_1 = j+1$, $\eta_x = 1$, $\eta_y = 0$.

In the limit $N \to \infty$ the fluctuations around the mean value become Gaussian, $\xi_j^{(N)}(t) \to \xi_j(t)$, and are governed by the linear, time-dependent Langevin equation

$$\frac{d}{dt}\xi_j(t) = \sum_{i=1}^{M} L_{ji}(\boldsymbol{\rho}(t))\, \xi_i(t) + W_j(t) \quad (2.14)$$

The matrix L_{ij} is obtained by linearizing (2.11) around the solution $\boldsymbol{\rho}(t)$. The fluctuating forces, W_j, are Gaussian with zero mean and covariance

$$\langle W_i(t)\, W_j(t') \rangle = \delta(t-t')\, g_{ij}(\boldsymbol{\rho}(t)) \quad (2.15)$$

The covariance g is the matrix of second jump moments for (2.7). It has the structure of a discrete Laplacian and is given by

$$g_{ij}(\boldsymbol{\rho}) = \delta_{ij}(a_i(\boldsymbol{\rho}) + a_{i-1}(\boldsymbol{\rho})) - \delta_{ij-1} a_i(\boldsymbol{\rho}) - \delta_{ij+1} a_{i-1}(\boldsymbol{\rho}) \quad (2.16)$$

with

$$a_j(\boldsymbol{\rho}) = R(\rho_{j-1}, \rho_j, \rho_{j+1}, \rho_{j+2}) + R(\rho_{j+2}, \rho_{j+1}, \rho_j, \rho_{j-1}) \quad (2.17)$$

Since we are interested in the steady state for (2.7), we would like to take the limit $t \to \infty$ in (2.11) and (2.14). As emphasized by van Kampen the linear Gaussian approximation is meaningful uniformly in time only if the solutions to (2.11) all tend to a common fixed point as $t \to \infty$. This condition breaks down at low temperatures. We will then have to use the theory of large deviations to extract some information on the steady state as $N \to \infty$.

At the boundaries, $j = 1$ and $j = M-1$, the currents J_j and the fluctuation strengths $g_{ij}(\rho)$ are modified through the closed end boundary conditions. Computationally this is cumbersome. Therefore from now on we consider the infinite system, $-\infty < j < \infty$, which we approximate through a finite system with periodic boundary conditions. This means $-M \leqslant j \leqslant M$ and $\rho_{M+1} = \rho_{-M}$, $\xi_{M+1} = \xi_{-M}$. The total number of columns is then $2M+1$. We expect that in general our order of limits, first $N \to \infty$ then $M \to \infty$, could be interchanged.

3. CRITICAL POINT, SPINODAL LINE, AND CRITICAL EXPONENTS

In the high-temperature regime, β small, the homogeneous states $\rho_i \equiv \rho$, $J_j = 0$ are the only stationary solutions of the deterministic evolution equation (2.11) with periodic boundary conditions. They are all stable. For given ρ the stationary distribution of the reduced master equation (2.7) for large N is then a Gaussian centered at the homogeneous state with a relative width of the order $N^{-1/2}$. Its covariance is given by the stationary solution of (2.14). To determine it we exploit the translation invariance of the homogeneous state and introduce the fluctuation modes

$$\hat{\xi}_k(t) = \sum_{n=-M}^{M} e^{ikn} \xi_n(t) \tag{3.1}$$

where the wave number k is in the first Brillouin zone, $-\pi \leqslant k \leqslant \pi$. In the limit $M \to \infty$, k becomes a continuous variable. The Langevin equations (2.14) decouple as

$$\frac{d}{dt} \hat{\xi}_k(t) = \hat{L}(k)\, \hat{\xi}_k(t) + \hat{W}(k, t) \tag{3.2}$$

Here

$$\begin{aligned} \hat{L}(k) &= -R_{23} - (R_{14} - R_{23}) \cos k + R_{14} \cos 2k \\ \langle \hat{W}(k, t)\, \hat{W}(k', t') \rangle &= \delta(k - k')\, \delta(t - t')\, \hat{g}(k) \\ \hat{g}(k) &= 2D(1 - \cos k) \end{aligned} \tag{3.3}$$

where

$$D(\rho) = R(\rho, \rho, \rho, \rho) \tag{3.4}$$

$$R_{ij}(\rho) = \left(\frac{\partial}{\partial x_i} R - \frac{\partial}{\partial x_j} R \right) \Bigg|_{x = \rho}, \qquad i, j = 1, \ldots, 4$$

With $\langle \xi_i \xi_j \rangle = G(i - j)$, the steady-state covariance, the structure function is given by

$$S(k) = \sum_n e^{ink} G(n) \tag{3.5}$$

and therefore

$$S(k) = -\frac{\hat{g}(k)}{2L(k)} = \frac{D}{R_{23} + R_{14}(1 + 2 \cos k)} \tag{3.6}$$

Due to the randomness of the particle distribution in each column, S is independent of the vertical component of the wave vector.

The homogeneous state with a given density ρ may lose its stability as the temperature $T=\beta^{-1}$ decreases and reaches some critical value $T_s(\rho)$, which, in the usual equilibrium mean field terminology, we call the spinodal temperature. This instability is connected with critical fluctuations and a diverging horizontal correlation length. Correspondingly the structure function $S(k)$ diverges at a certain wave number k_c characterizing the critical fluctuations. For attractive intercolumn ($J_h>0$) the instability will be driven by spatially homogeneous fluctuations, $k_c=0$, while for repulsive interactions ($J_h<0$) the critical fluctuations are staggered, $k_c=\pi$. The spinodal temperature $T_s(\rho)$ is thus determined by

$$R_{23}+3R_{14}=0, \qquad \text{for} \quad J_h>0 \tag{3.7a}$$

$$R_{23}-R_{14}=0, \qquad \text{for} \quad J_h<0 \tag{3.7b}$$

and R_{14} vanishes for $J_h=0$.

By the particle–hole symmetry of the lattice gas, which is preserved by our dynamics,[2] the instability curve $T_s(\rho)$ in the ρ–T plane is symmetric around $\rho=\frac{1}{2}$ and takes its maximum at $\rho=\frac{1}{2}$. Hence $\rho_c=\frac{1}{2}$, $T_c=T_s(\frac{1}{2})$ is the critical point of the system. Its properties are studied in this section.

The occurence of a spinodal depends on the choice of the rate function $\phi_\perp$. For attractive, isotropic couplings, $J_h=J_v=J>0$, there is a transition for all $\phi_\perp$, whereas for repulsive couplings, $J_h=J_v<0$, the transition is completely suppressed. To discuss mixed couplings we assume a monotone decreasing rate function $\phi_\perp$, normalized as $\phi_\perp(0)=1$ and having a limiting value

$$\varepsilon=\lim_{x\to-\infty}\phi_\perp(x) \tag{3.8}$$

$1\leqslant\varepsilon\leqslant\infty$. Then for $-J_h=J_v>0$ (resp., $J_h=0$, $J_v>0$), a phase transition exists only if $\varepsilon>\frac{5}{2}$ (resp., $\varepsilon>\frac{9}{2}$).[24]

To understand the rate dependence of the critical temperature in the attractive isotropic case we calculate T_c for four different rate functions $\phi_\perp$ as given in the first column of Table I. We note that the rate functions and their corresponding critical temperatures T_c are ordered increasingly. Furthermore, in general, $T_c=1/\beta_c$ satisfies

$$0.14\leqslant\beta_c J\leqslant 0.43 \tag{3.9}$$

(see Ref. 24). The equilibrium critical temperature of the two-dimensional lattice gas is $\beta_c J=0.44$ according to Onsager. Thus we find a rise in the

Table I. Critical Temperature for Attractive Isotropic Couplings

Rate function $\phi(x)$	ε [cf. (3.8)]	$\beta_c J = J/kT_c$
$\phi_0(x) = \begin{cases} e^{-x} & x > 0 \\ 1 & x \leqslant 0 \end{cases}$	1	0.43
$\phi_1(x) = \dfrac{2}{1+e^x}$	2	0.25
$\phi_2(x) = e^{-x/2}$	∞	0.20
$\phi_\infty(x) = \begin{cases} 1 & x > 0 \\ e^{-x} & x \leqslant 0 \end{cases}$	∞	0.15

critical temperature, as compared to equilibrium, for any realization of our model. The same trend is found in the numerical simulations.[2,7,8] We have $\beta_c J \cong 0.32$.[2] It thus appears that the fast-rate limit lowers the critical temperature. This is further confirmed by a Monte Carlo simulation for $\gamma = \Gamma_\parallel/\Gamma_\perp = 1, 5, 20$, and 80 on a 50×50 lattice for which the critical temperature is found to decrease as a function of γ.[7]

In fact, for higher dimension ($d \geqslant 3$), the fast-rate limit with Metropolis rates gives critical temperatures lower than the corresponding equilibrium ones; while, with vBS rates, they are higher. The d-dependences of β_c's are given by

$$\frac{d-(1+d)\,e^{-4\beta_c^M J}}{2^{4d-4}} \sum_{n=0}^{2d-2} \binom{4d-3}{n} e^{-4\beta_c^M J(2d-2-n)} = 1 \tag{3.10}$$

and

$$(2d+1)\tanh(\beta_c^{\mathrm{vBS}} J) = 1 \tag{3.11}$$

As a common trend, T_c grows with d in both cases and asymptotically tends to the mean field behavior, i.e., $\beta_c \sim 1/2d$, as $d \to \infty$.

We proceed to determine the critical exponents in the case of attractive interactions. The left-hand side of (3.7a), evaluated at $\rho_c = \frac{1}{2}$, has a nonvanishing derivative with respect to temperature. The divergence of the forward scattering cross section, $S(0)$, at the critical point is therefore given by

$$\begin{aligned} S(k) &\simeq |T - T_c|^{-1} \qquad \text{for} \quad k = 0,\ T \to T_c \\ S(k) &\simeq k^{-2} \qquad\qquad\ \text{for} \quad T = T_c,\ k \to 0 \end{aligned} \tag{3.12}$$

The exponents γ and η thus take on their classical values $\gamma = 1$ and $\eta = 0$. The pair correlation function decays exponentially as

$$G(n) = G(0)\, e^{-|n|/\xi} \tag{3.13}$$

on a length scale $\xi \simeq ((T - T_c)/T_c)^{-1/2}$ as T approaches T_c. Thus we find the classical value $\nu = \frac{1}{2}$ for the exponent of the correlation length. The prefactor

$$G(0) = \langle \xi_j^2 \rangle \tag{3.14}$$

in (3.13) diverges also as $((T - T_c)/T_c)^{-1/2}$. Since $\langle \xi_j^2 \rangle = 1/N$ $(\langle n_j^2 \rangle - \langle n_j \rangle^2)$, this implies that in the limit $N \to \infty$ the density fluctuations in each column diverge at T_c.

The critical exponent α related to the specific heat has no unique definition in the present nonequilibrium situation. In equilibrium C_v can be expressed in a variety of ways such as the derivative of the internal energy with respect to temperature, the second derivative of the free energy or energy fluctuations, and so forth. In nonequilibrium, these different definitions do not have to coincide. If we adopt the fluctuation–response relation, then

$$\tilde{C}_v = \frac{1}{k_B T^2} |\Lambda|^{-1} (\langle H^2 \rangle - \langle H \rangle^2) \tag{3.15}$$

$\langle H \rangle$ and $\langle H^2 \rangle$ are calculated from (2.1) by first averaging the site occupation variable η_x over the uniform distribution with fixed $\mathbf{n}$ and then averaging $\mathbf{n}$ over the Gaussian distribution with covariance (3.6). We find that $\tilde{C}_v$ diverges as $|T - T_c|^{-1}$ at the critical oint. On the other hand, the average energy shows no temperature dependence above T_c.[9] There is, however, a quasi-one-dimensional correction term, $\simeq N^{-1}((T - T_c)/T_c)^{-3/2}$, to $\tilde{C}_v$ corresponding to a similar contribution, $\simeq N^{-1}((T - T_c)/T_c)^{-1/2}$, to the average energy. For the vBS model the average current, $\langle J \rangle$, is proportional to $\langle H \rangle$. Therefore $d\langle J \rangle/dT$ has a jump at T_c in accordance with the numerical simulations.[2,6]

Finally, let us determine the dynamical exponent z of our model. Each fluctuation mode $\xi_k(t)$ has a relaxation time $\tau_k = -\hat{L}(k)^{-1}$. The mode connected with the critical wave number k_c slows down as

$$\tau_k \simeq |k - k_c|^{-z} \qquad \text{at} \quad T = T_c, k \to k_c \tag{3.16}$$

Therefore

$$\begin{aligned} z &= 4 \quad \text{for} \quad J_h > 0 \\ z &= 2 \quad \text{for} \quad J_h < 0 \end{aligned} \tag{3.17}$$

For attractive horizontal interaction the order parameter is conserved, which leads to $z=4$, whereas the staggered density distribution emerging in the repulsive case corresponds to a nonconserved order parameter. Equation (3.17) agrees with the classical van Hove theory of critical slowing down. For $J_h=0$ the structure function $S(k)$ is independent of k, which means that all modes lose their stability simultaneously. There is then no critical wave number k_c and no critical slowing down in the sense of (3.16).

4. PHASE COEXISTENCE

Having discussed the high-temperature regie and the critical point, we would like to understand the low-temperature behavior of the driven lattice gas. From now on only attractive isotropic couplings, $J>0$, are considered. As observed in Monte Carlo simulations, the system segregates into a low- and a high-density phase. Our first goal is to determine this phase coexistence curve for the vBS model.

As noted in Ref. 9, for the jum rates $\phi_\perp=\phi_2$ and for the couplings $J_v>0$, $J_h=0$ the steady-state distribution, and therefore the phase coexistence curve, is obtainable exactly. Since our analysis of the isotropic case is motivated by this particular solution, we first describe its structure for large N. The steady-state distribution is approximately given by

$$p^{(N)}(\mathbf{n})=Z^{-1}\exp[-N\cdot F(\boldsymbol{\rho})]\,\delta\left(\sum_{j=-M}^{M}\rho_j-(2M+1)\,\rho\right) \tag{4.1}$$

with $\rho_j=n_j/N$, where $F(\rho)$, which can be thought of as a "free energy" functional, has the form

$$F(\boldsymbol{\rho})=\sum_{j=-M}^{M} f(\rho_j) \tag{4.2}$$

with

$$f(\rho)=2\int_0^\rho d\lambda\,\log((\lambda\exp[-2\beta J_v]+1-\lambda)/(1-\lambda)$$
$$\times\exp[-2\beta J_v]+\lambda))+\rho\log\rho+(1-\rho)\log(1-\rho) \tag{4.3}$$

Furthermore the current J_j in (2.12) can be written in the form

$$J_j(\boldsymbol{\rho})=-L_j(\boldsymbol{\rho})\left(\frac{\partial F}{\partial\rho_{j+1}}-\frac{\partial F}{\partial\rho_j}\right) \tag{4.4}$$

with strictly positive Onsager coefficients $L_j(\boldsymbol{\rho})$. Therefore $J_j(\boldsymbol{\rho})=0$ is equivalent to

$$\frac{\partial F}{\partial \rho_{j+1}}=\frac{\partial F}{\partial \rho_j}=C \tag{4.5}$$

independent of j, $j=-M,\ldots,M$, which defines precisely the stationary points of F under the constraint $\sum_j \rho_j=(2M+1)\,\rho$. Thus time-independent solutions of (2.11) with zero current coincide with stationary oints of F under the constraint $\sum_j \rho_j=(2M+1)\,\rho$.

The structural similarity with eqilibrium mean field models is quite apparent. We want to introduce briefly one such model because it will be useful for the understanding of the low-temperature static solutions, cf. Sec. 5. As in the vBS model, particles jump on a $(2M+1)\times N$ square lattice with periodic boundary conditions. The Hamiltonian is of mean field type

$$H=-4J\frac{1}{N}\sum_{j=-M}^{M}(n_j n_{j+1}+n_j^2) \tag{4.6}$$

with n_j the number of particles in the jth column, $0\leqslant n_j\leqslant N$, $n_{-M}=n_{M+1}$. The jumps are assumed to satisfy detailed balance with respect to H. Then, independently of the jump rates, the steady-state distribution is $Z^{-1}\exp[-\beta H]\,\delta(\sum_{j=-M}^{M} n_j-N(2M+1)\,\rho)$ which for large N is of the form (4.3) with the free energy functional

$$\begin{aligned}F_{\mathrm{eq}}(\boldsymbol{\rho})=&-4\beta J\sum_{j=-M}^{M}(\rho_j\rho_{j+1}+\rho_j^2)\\&\sum_{j=-M}^{M}(\rho_j\log\rho_j+(1-\rho_j)\log(1-\rho_j))\end{aligned} \tag{4.7}$$

$\rho_{M+1}=\rho_{-M}$. As in the vBS model, the time-dependent densities $\rho_j^{(N)}(t)=n_j(t)/N$ become deterministic for large N and are governed by

$$\frac{d}{dt}\rho_j(t)+J_j(\boldsymbol{\rho}(t))-J_{j-1}(\boldsymbol{\rho}(t))=0 \tag{4.8}$$

where J_j is of the form (4.4) with F replaced by F_{eq} and with Onsager coefficients depending on the specific choice of the jump rates.

We return to the driven lattice gas for general jump rates and isotropic couplings. In analogy to the cases just discussed we *assume* that the steady state for large N is of the form

$$p^{(N)}(\mathbf{n})=Z^{-1}\exp[-NF(\rho)]\,\delta\left(\sum_{j=-M}^{M}\rho_j-(2M+1)\,\rho\right) \tag{4.9}$$

with a suitable "free energy" F which is not known explicitly. Since detailed balance is not satisfied, there is no reason to believe that F is related to the current by (4.4). Still for small noise, i.e., large N, the system will spend a long time near stationary dynamically stable solutions of (2.11) and these should be reflected as local minima of F. Thus an investigation of the deterministic dynamics yield indirectly some information on F. This will be pursued in Sec. 5.

Here we determine the phase coexistence curve for $M \to \infty$ by a purely static argument analogous to that used in Ref. 9. Assuming the form (4.9) we define a function, μ, by

$$\beta\mu(\rho) = \frac{\partial}{\partial \rho_0} F \Big|_{\{\rho_m = \rho\}} \tag{4.10}$$

where by symmetry the differentiation could be with respect to any ρ_j. Now, for ρ in the stable regime,

$$\begin{aligned} \frac{\partial}{\partial \rho} \beta\mu(\rho) &= \sum_j \frac{\partial^2}{\partial \rho_j \, \partial \rho_0} F \Big|_{\{\rho_m = \rho\}} \\ &= S^{-1}(0)(\rho) = (R_{23}(\rho) + 3R_{14}(\rho))/D(\rho) \end{aligned} \tag{4.11}$$

The second equality follows from considering the (small) Gaussian fluctuations about the uniform state. From (4.9) these are obtained as

$$\{\langle \xi_i \xi_j \rangle\}^{-1} = \frac{\partial^2}{\partial \rho_i \, \partial \rho_j} F \Big|_{\{\rho_m = \rho\}} \tag{4.12}$$

where $\{\cdot\}^{-1}$ denotes the inverse of the covariance matrix which we know from the Ω-expansion, cf. (3.5), (3.6). Solving (4.11) for μ as a function of ρ, we find that μ has a form well known from the van der Waals gas. Below T_c, when analytically continued inside the spinodal, μ has a double loop structure. Evaluating then $F(\rho)$ for $\rho_i = \rho$, we see that it has a double minimum for $T < T_c$, symmetric around $\rho\frac{1}{2}$. The phase coexistence curve is then identified with these minima of F, obtained with uniform ρ_j's according to (4.9). This is of course equivalent to the Maxwell construction in equilibrium.

In Figure 1 we plot the coexistence and spinodal curves for the horizontal rate functions ϕ_0 and ϕ_2 of Table I. A typical feature of the phase diagram for rate functions characterized by $\varepsilon < \infty$ [cf. (3.8)] is that both the coexistence and the spinodal curves hit the $T = 0$ axis at values of ρ different from 0 and 1. Consequently, if the lattice gas is sufficiently dilute (or dense), the homogeneous state remains stable all the way to zero

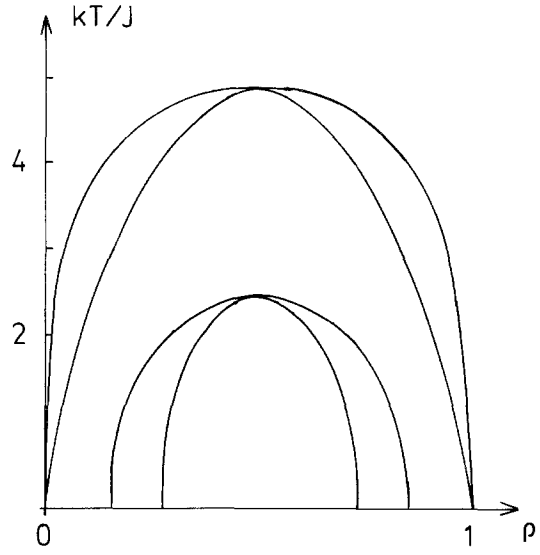

Fig. 1. Phase coexistence and sinodal curves in the case of isotropic, attractive couplings for the vBS rates (upper curves) and for the Metropolis rates (lower curves).

temperature for these rates. (This does not happen of course for the equilibrium system, $\mathbf{E} = 0$.)

What has been done here, beyond the explicit assumption of the N dependence of $p^{(N)}(\mathbf{n})$ in (4.9), is:

(i) Assume that for large M we can let $k \to 0$ in (3.6) to obtain the last equality in (4.11). This is related to the equivalence of the canonical and grand canonical ensembles which can be proven for equilibrium. We implicitly assumed this equivalence in the analysis (4.9)–(4.12), since in fact F of (4.9) is not unique with respect to addition of an arbitrary function $\psi_M(\sum_{j=-M}^{M} \rho_j)$. The implicit physical assumption is that distant columns should not be coupled directly through $p^{(N)}(\mathbf{n})$ which translates into assuming that ψ_M can only be linear in its argument. [Of course we also assume that F is well behaved as, for example, in (4.7).]

(ii) Assume that the covariance of small fluctuations about an initially uniform state, given by the Ω-expansion, is meaningful for the description of the stationary state inside the spinodal where in fact the uniform state is unstable. Put alternatively, this means that $S^{-1}(0)$ can be meaningfully continued inside the spinodal to obtain global information about F. The coexistence curve which is outside the spinodal curve then marks the region, according to this construction, where the uniform state is no longer stable against large deviations, i.e., against splitting into two

phases. Thus, *a posteriori*, we are not justified in using the Ω-expansion even in this region. So why should this construction have any validity for describing the large N behavior of stationary solutions of the master equation (2.7)?

One possible justification is based on the observation that for equilibrium systems, such as the model (4.6), the Maxwell construction has also a dynamical meaning. We fix a temperature T below T_c and look for a stationary, zero current, and dynamically stable solution ρ_j to (4.8) such that

$$\lim_{j \to \pm\infty} \rho_j = \rho_\pm \tag{4.13}$$

and such that ρ_j increases monotonically. There exists, up to translations, only one such kink solution, and the asymptotic densities, ρ_+ and ρ_-, are exactly on the coexistence curve, cf. Sec. 5.4. Physically this solution corresponds to the segregation into two phases. If the Maxwell construction is to be meaningful also in our nonequilibrium context, then its result has to agree with the dynamical determination of the phase coexistence curve. Unfortunately, we could not find the kink solution to (2.11) analytically. For the particular case of the rates ϕ_2 we obtained the kink solutions numerically. Their construction will be explained in the following section. Within some temperature interval below T_c, their asymptotic densities ρ_+ and ρ_- lie on the phase coexistence curve as obtained from the Maxwell construction, cf. Table III. Therefore it appears that the Maxwell

Table II. Numerical Construction of the Kink Solution[a]

$\tau = \frac{K_c - K}{K_c}$	$N_{1/2}$	$2\rho_{max} - 1$	$2\rho_{ph} - 1$	$2\rho_s - 1$
5×10^{-4}	31.0	0.0395	0.0395	0.0228
2.5×10^{-3}	13.9	0.0882	0.0882	0.0510
5×10^{-3}	9.8	0.1244	0.1244	0.0720
0.01	7.0	0.1752	0.1752	0.1016
0.024	4.4	0.2733	0.2733	0.1595
0.09	2.2	0.5102	0.5127	0.3084
0.17	—	0.6412	0.6705	0.4184
0.33	—	0.6763	0.8711	0.5955
0.5	—	0.6931	0.9666	0.7372

[a] Columns: (1) Reduced temperature; K defined by (5.11). (2) Half width of kink in units of the lattice spacing. (3) Maximal density of kink, cf. Sec. 5.5. (4) Phase coexistence curve as calculated from (4.11). (5) Spinodal as calculated from (5.20).

construction is the correct procedure also for the stationary distribution of (2.7) in the limit $N \to \infty$. To some extent this justifies also our ansatz (4.9).

We are now in a position to determine the critical exponents β and δ related to the order parameter $\rho - \rho_c$. In the vicinity of the critical point, $S^{-1}(0)$ is of the form

$$S^{-1}(0) = A + B(\rho - \rho_c)^2 \tag{4.14}$$

$A = A_0(T - T_c)$; A_0, $B > 0$. Integrating twice with respect to ρ yields the free energy per site

$$f(\rho) = f_0 + \tfrac{1}{2}A(\rho - \rho_c)^2 + \frac{1}{12}B(\rho - \rho_c)^4 \tag{4.15}$$

which has the form of the conventional Landau free energy. The critical exponents thus take on their classical values $\beta = \frac{1}{2}$, $\delta = 3$.

From $S(k)$ we can also determine a surface tension. In equilibrium the Ginzburg–Landau free energy functional is[23]

$$F(\{\rho(x)\}) = \int dx \left[\kappa \left(\frac{d}{dx} \rho \right)^2 + f(\rho(x)) \right] \tag{4.16}$$

Below T_c, F is minimized by the usual kink profile

$$(\rho(x) - \rho_c) = (-3A/B)^{1/2} \tanh \left[\left(-\frac{A}{2\kappa} \right)^{1/2} x \right] \tag{4.17}$$

where the interface position is arbitrarily fixed at $x = 0$. Equation (4.17) shows that the width of the interface diverges as $((T_c - T)/T_c)^{-1/2}$ at the critical point. The surface tension σ, which coincides with the surface part of the free energy in this one-dimensional case, is obtained by evaluating (4.16) at the stationary profile (4.17). This yields

$$\sigma = (\sqrt{2}/3B)\, \kappa^{1/2} A^{3/2} \tag{4.18}$$

To determine the surface tension in our model, we have to find an expression for κ. In mean field approximation the static fluctuations in the homogeneous state of (4.16) are given by the second derivative of F at the corresponding density and therefore

$$S(k) = \frac{1}{f''(\rho) + \kappa(\rho)\, k^2} \tag{4.19}$$

We compare with (3.6). The $k = 0$ contribution agrees by construction. It is therefore tempting to identify the term of order k^2 with κ. This yields

$$\kappa(\rho) = -R_{14}(\rho)/D(\rho) \tag{4.20}$$

κ is strictly positive for all T and $\sigma \sim (T_c - T)^{3/2}$ as in mean field.

5. THE ASSOCIATED DISCRETE DYNAMICAL SYSTEM

As a next step we want to determine stationary, nonhomogeneous solutions of (2.11). We are interested in them for several reasons. First, as already mentioned, there should be among them dynamically stable kink solutions with asymptotic densities on the phase coexistence curve. These will hopefully coincide with those obtained from the Maxwell construction used before. Second, as explained in Sec. 4, dynamically stable, zero-current solutions should correspond to local minima of F, cf. (4.9). Therefore it should be possible to identify these solutions as metastable/stable configurations of the system. Such long-lived configurations have been observed in Monte Carlo simulations.[2,7] This information about inhomogeneous stationary states is clearly not obtainable via the methods used for determining $F(\boldsymbol{\rho})|_{\rho_l=\rho}$ in the preceding section. If we could identify all stationary, dynamically stable solutions of (2.11), we would have a tool to go beyond the Ω-expansion and to understand, at least in principle, the long time dynamics and the stationary distribution for large N also in the low-temperature regime.

Let us fix some finite M and the temperature T of the system. We label the stationary, dynamically stable solutions of (2.11) as $\{\boldsymbol{\rho}_l, l=1,..., L\}$. We assume that (2.11) has an attracting set of a simple structure. To each $\boldsymbol{\rho}_l$ there is a basin of attraction, Γ_l, and $\bigcup_l \Gamma_l$ exhausts the phase space $[0, 1]^M$ up to hypersurfaces of codimension one. $\mathbf{n}(t)/N$ as governed by the master equation (2.7) is deterministic with a small noise of order $N^{-1/2}$. We picture then its dynamics in the following way: $\mathbf{n}(t)/N$ spends a long time near a particular stationary solution, say $\boldsymbol{\rho}_l$. The fluctuations around $\boldsymbol{\rho}_l$ are governed by a Langevin equation of the form (2.14). Through an unlikely fluctuation ($\equiv$ large deviation) $\mathbf{n}(t)/N$ jumps to some other stationary solution, say $\boldsymbol{\rho}_{l'}$, etc. The theory of Freidlin and Wentzell on sall random perturbations of dynaical systems[26] determines the transition rates

$$K(l, l') = e^{-NV(l,l')} \tag{5.1}$$

from the stationary configuration $\boldsymbol{\rho}_l$ to the stationary configuration $\boldsymbol{\rho}_{l'}$. For the equilibrium model of Sec. 4, $V(l, l')$ is related to the minimal free energy barrier between $\boldsymbol{\rho}_l$ and $\boldsymbol{\rho}_{l'}$. If detailed balance is not satisfied, $V(l, l')$ is obtained as the solution of some complicated variational problem. Let $p(l)$ denote the stationary distribution for the master equation with the rates $K(l, l')$. For large N it is of the form

$$p(l) = Z^{-1} \exp[-Nf(l)] \tag{5.2}$$

$p(l)$ is then the weight of the basin of attraction Γ_l with respect to the stationary distribution $p^{(N)}$ of (2.7). $p^{(N)}$ close to $\boldsymbol{\rho}_l$ is approximately

Gaussian with a covariance determined by a Langevin equation as in the homogeneous high-temperature case discussed before. $f(l) = F(\boldsymbol{\rho}_l)$ with F of (4.9) is the "free energy" of the configuration $\boldsymbol{\rho}_l$.

Our analysis of the stationary solutions to (2.11) is rather modest. We obtain periodic solutions and discuss their stability. The kink solution is found numerically. For 8 columns ($M = 8$) we carry through approximately the Freidlin–Wentzell theory and determine the jump rates $K(l, l')$ and the free energies $f(l)$.

5.1. The Discrete Mapping

The stationary, zero-current solutions of (2.11) can be obtained as the trajectories of a discrete dynamical system. We require the current (2.12) to vanish, which yields

$$R(\rho_{j-1}, \rho_j, \rho_{j+1}, \rho_{j+2}) = R(\rho_{j+2}, \rho_{j+1}, \rho_j, \rho_{j-1}) \tag{5.3}$$

For the rate function $\phi_\perp(x) = \phi_2(x) = e^{-x/2}$ these recurrence relations take a particularly convenient form. We simplify them further by introducing the variables

$$\begin{aligned} a_j &= (\rho_j + b(1-\rho_j))/b\rho_j + 1 - \rho_j) \\ b &= e^{-2\beta J} \end{aligned} \tag{5.4}$$

and only consider the case $J_h = J_v = J > 0$. In terms of the a_j's, the condition of zero current reads then

$$\begin{aligned} a_j &= G(a_{j-3}, a_{j-2}, a_{j-1}) \\ G(x, y, z) &= x \frac{y^2(y-b)(1-bz)}{z^2(z-b)(1-by)} \end{aligned} \tag{5.5}$$

This is equivalent to the trajectories of the discrete map

$$\hat{T}(z_1, z_2, z_3) = (z_2, z_3, G(z_1, z_2, z_3)) \tag{5.6}$$

The physical domain in $\mathbf{z}$-space is restricted by $b \leqslant z_i \leqslant b^{-1}$. The nonlinear maping $\hat{T}$ does not preserve volume, $\det(\partial \hat{T}/\partial \mathbf{z}) \neq 1$ except for some specific values of $\mathbf{z}$. The dynamical system (5.6) is reversible in the sense that

$$a_j = G(a_{j+3}, a_{j+2}, a_{j+1}) \tag{5.7}$$

for any trajectory $\{a_j\}$ satisfying (5.5). We are thus dealing with a non-Hamiltonian, reversible dynamical system similar to the one considered in Ref. 21 in the context of classical spin chains.

5.2. Fixed Points

The general structure of $\hat{T}$ implies that any fixed point must be located on the diagonal $z_1 = z_2 = z_3$. Indeed, the diagonal represents a whole line of fixed points, corresponding to the homogeneous stationary solutions of (2.11). The character of the fixed points is determined by the sinodal curve of the lattice gas. Consider the linearization $D\hat{T}|_\alpha$ of $\hat{T}$ at the fixed point $z_i = \alpha$, $i = 1, 2, 3$, where $\alpha = \alpha(\rho)$ is related to the density ρ of the associated homogeneous state by (5.4). $D\hat{T}|_\alpha$ is volume preserving, $\det(D\hat{T}|_\alpha) = 1$. One of its eigenvalues, denoted by λ_0, is always equal to unity, with the corresponding eigenvector pointing along the diagonal. This reflects the marginal homogeneous ($\mathbf{k} = 0$) fluctuation ode in (3.2). The remaining two eigenvalues λ_+ and λ_- must then satisfy

$$\lambda_+ \cdot \lambda_- = 1 \tag{5.8}$$

which admits the following four cases:

$$\begin{aligned}
&\text{(i)} \quad \lambda_+ = \lambda_- = 1 \qquad \text{(parabolic)} \\
&\text{(ii)} \quad \lambda_+, \lambda_- \in \mathbb{R};\ \lambda_+ > \lambda_- > 0 \qquad \text{(hyperbolic)} \\
&\text{(iii)} \quad \lambda_+, \lambda_- \in \mathbb{R};\ \lambda_+ < \lambda_- < 0 \qquad \text{(hyperbolic with reflection)} \\
&\text{(iv)} \quad \lambda_\pm = e^{\pm i\Theta},\ \Theta \in (0, 2\pi) \qquad \text{(elliptic)}
\end{aligned} \tag{5.9}$$

For a given temperature T, the fixed point $\{z_i \equiv \alpha(\rho)\}$ is elliptic if ρ lies in the spinodal interval, hyperbolic if ρ lies outside, and parabolic if ρ is on the spinodal.

This indicates a remarkable connection between the notions of stability in the two distinct dynamical systems (2.11) and (5.6). If ρ lies inside (outside) the spinodal interval, the homogeneous solution to (2.11) with density ρ is dynamically unstable (stable), whereas the corresponding fixed point of $\hat{T}$ is elliptic (hyperbolic) and therefore stable (unstable). This relationship is readily generalized to the n-cycles of (5.6), i.e., to trajectories with period n. For a detailed discussion of the general case we refer the reader to Ref. 20. Their arguments apply to our model in a very similar way.

The fact that, generally speaking, configurations of physical interest correspond to unstable trajectories of the associated discrete dynamical system has been commonly recognized. As a consequence, the actual location of such trajectories poses great numerical difficulties.[17] We therefore focus our attention on simple, small-period cycles of the discrete dynamical system, which are accessible to analytic calculations and which will provide us already with considerable insight into the low-temperature

structure. We want to stress, however, that the overall picture to be developed below by no means exhausts the diversity of configurations generated by the maping (5.6).

5.3. Periodic Trajectories

Cycles with small periods ($n = 3, 4, 6, 8$) are obtained analytically from the recursion relation (5.5) by taking an appropriate ansatz for the trajectory. We note that the particle–hole transformation $\rho_j \to 1 - \rho_j$ of the column densities ρ_j corresponds to $a_j \to a_j^{-1}$ in the variables of (5.4). Thus a 4-cycle $\{a_j\}$ with the corresponding configuration $\{\rho_j\}$ being symmetric with respect to the critical density $\rho_c = \frac{1}{2}$ is of the form

$$\{a_j\} = (..., \alpha, \alpha, \alpha^{-1}, \alpha^{-1}, \alpha, \alpha, \alpha^{-1}, ...) \tag{5.10}$$

Inserting this into (5.5) yields a nonlinear equation for α, which develops a nontrivial solution ($\alpha \neq 1$) below a characteristic temperature $T^{(4)} < T_c$, where the superscrit denotes the periodicity of the cycle. We introduce the temperature parameter

$$K = \cot h\beta J \tag{5.11}$$

which is unity at $T = 0$ and increases monotonically with T. On its scale the

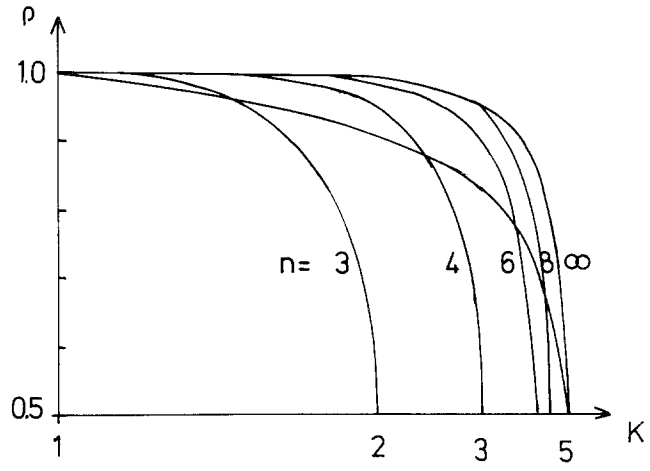

Fig. 2. Maximal density versus temperature for solutions with periods $n = 3, 4, 6, 8$. These solutions are dynamically stable only in between the spinodal and phase coexistence curves. The intersections with $\rho = \rho_c = \frac{1}{2}$ accumulate as $1/n^2$ at $K_c = 5$.

critical temperature is located at $K_c = 5$. Then $K^{(4)} = 3$, and for $K < K^{(4)}$ the configuration corresponding to (5.9) is given by

$$\begin{aligned} \{\rho_j - \rho_c\} &= \tfrac{1}{2}(..., v, v, -v, -v, v, v, ...) \\ v^2 = (v^{(4)})^2 &= K^2 \frac{(K^{(4)} - K)}{(3K-1)} \end{aligned} \tag{5.12}$$

Similarly a 3-cycle emerges at $K^{(3)} = 2$, with the corresponding configuation given by

$$\begin{aligned} \{\rho_j - \rho_c\} &= \tfrac{1}{2}(..., v, v, -v, v, v, -v, ...) \\ v^2 = (v^{(3)})^2 &:= K(K^{(3)} - K) \end{aligned} \tag{5.13}$$

For $n = 6$ and $n = 8$ the nontrivial n-cycles emerge at $K^{(6)} = 4$ and $K^{(8)} = 3 + \sqrt{2}$, respectively. The corresponding configurations do not have the simple structure as in (5.11) and (5.12). Qualitatively, they look like the period four configuration (5.11), i.e., they consist of a sequence of kinks and antikinks, each extending over $n/2$ lattice spacings (cf. Fig. 4).

For each of these n-cycles there is a simple relationship between the characteristic temperature $K^{(n)}$ and the eigenvalues $\lambda_\pm$ of the "critical" fixed point $\{z_i \equiv 1\}$, corresponding to the homogeneous state with critical density $\rho_c = \frac{1}{2}$. Below K_c, these eigenvalues are located on the unit circle. The angle Θ introduced in (5.9) is given by

$$\Theta(K) = \arccos\left(\frac{K-3}{2}\right) \tag{5.14}$$

for $K < K_c$; $\Theta(K_c) = 0$. Evaluating this expression at the characteristic temperature $K^{(n)}$ yields

$$\Theta(K^{(n)}) = \frac{2\pi}{n} \tag{5.15}$$

for $n = 3, 4, 6$, and 8. Thus the condition for an n-cycle to emerge is that all the eigenvalues of $D(\hat{T}^n) = (D\hat{T})^n$ at the "critical" fixed point coincide, i.e.,

$$(\lambda_\pm)^n = (e^{\pm i\Theta})^n = 1 = \lambda_0^n \tag{5.16}$$

at $K = K^{(n)}$.

We conjecture then that, for any integer $n \geqslant 3$, the "citical" fixed point of $\hat{T}$ emits an n-cycle of the mapping at the characteristic temperature

$$K^{(n)} = 3 + 2\cos\frac{2\pi}{n} \tag{5.17}$$

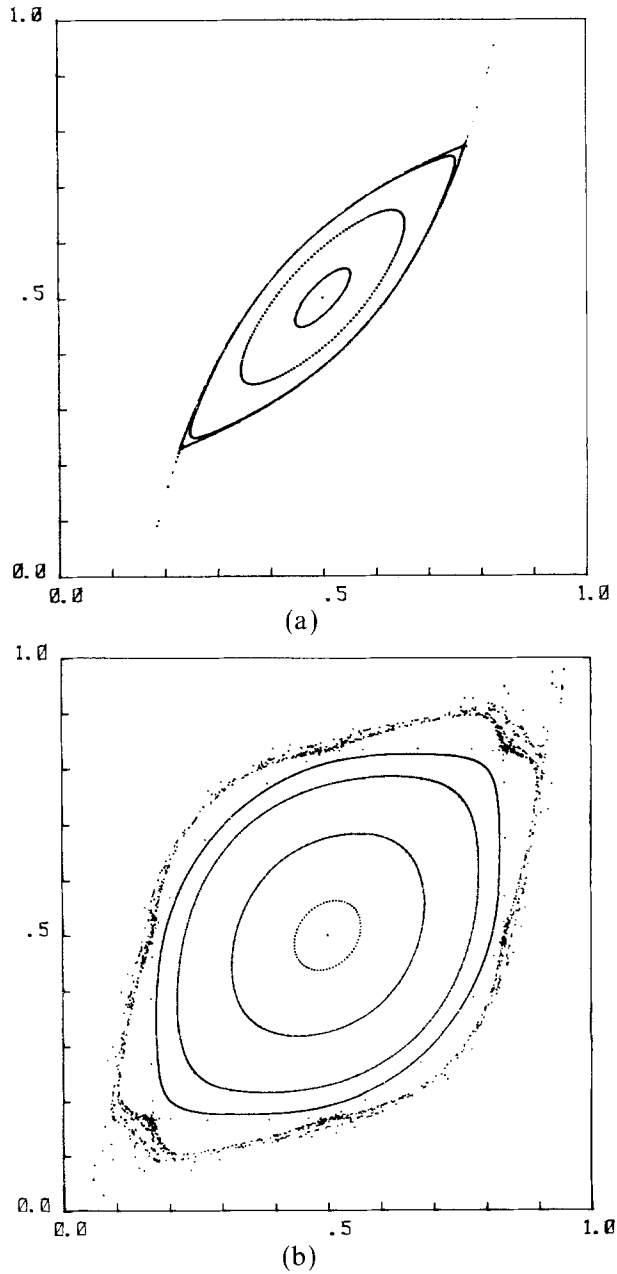

Fig. 3. Iterates of the map (5.21). (a) $\beta J = 0.28$, asymptotic densities of the kink solution $\rho_+ = 0.771$ and $\rho_- = 0.229$; (b) $\beta J = 0.4$, $\rho_+ = 0.945$, $\rho_- = 0.055$; (c) $\beta J = 0.6$, $\rho_+ = 0.991$, $\rho_- = 0.009$.

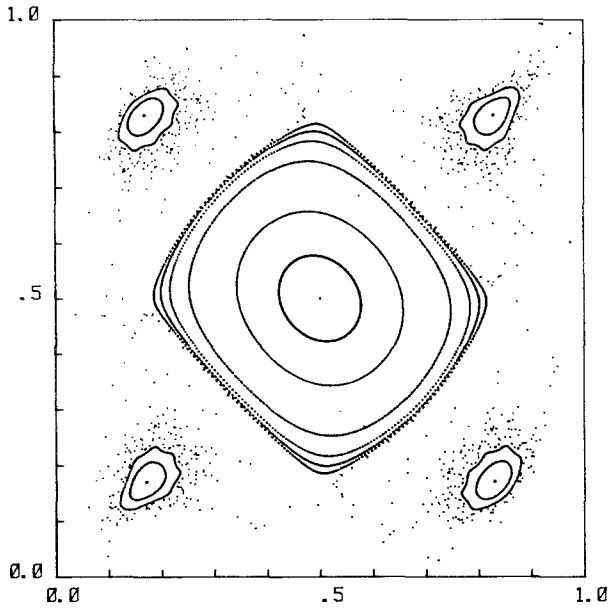

(c)

Fig. 3 (*continued*)

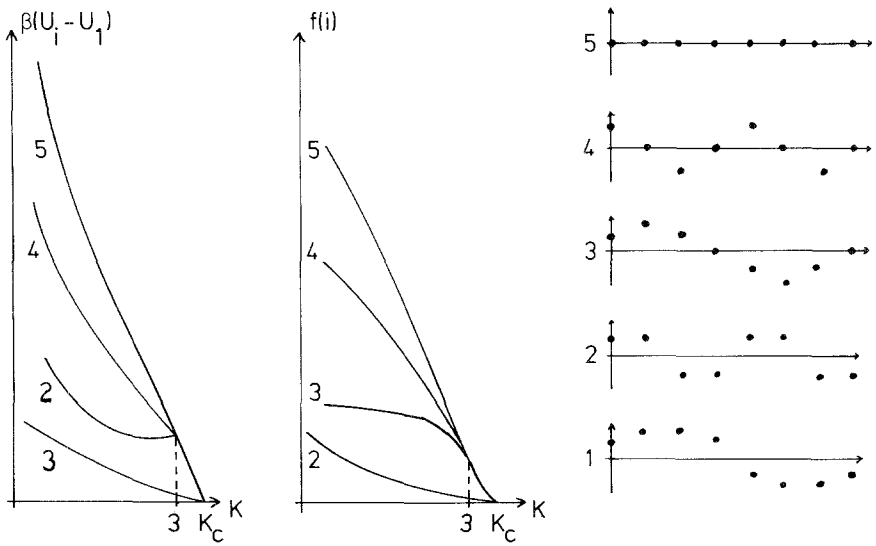

Fig. 4. Stable and metastable configurations of the eight-column system. The left (right) hand graph shows their energies (free energies) as a function of the temperature.

As $n \to \infty$, $K^{(n)}$ tends to $K_c = 5$ as $1/n^2$. The density configuration corresponding to the n-cycle consists of a sequence of kinks and antikinks, similar to the structure in (5.12), and its amplitude $v = |\rho_j - \rho_c|$ vanishes at $K^{(n)}$ as

$$v^2 \propto K^{(n)} - K \tag{5.18}$$

For $n = 2$, (5.17) yields $K^{(2)} = 1$, i.e., $T^{(2)} = 0$, implying that a staggered density configuration does not exist at finite temperatures.

Until now nothing has been said about the dynamical stability of the modulated density configurations emerging below T_c in our model, let alone about their statistical weight in the limit $N \to \infty$, which is crucial for the construction of a proper phase diagram. The local stability analysis can be carried out explicitly in the case of the 3- and 4-cycles given by (5.12) and (5.13). One finds that the corresponding states are stable below a certain temperature $K_s^{(n)} < K^{(n)}$, which is determined by the intersection of the density $v^{(n)}(K)$ of the n-periodic configuration and the spinodal, i.e., by the condition

$$v^{(n)}(K_s^{(n)}) = v_s(K_s^{(n)}) \quad (n = 3, 4) \tag{5.19}$$

where

$$v_s^2(K) = K \frac{K_c - K}{5K - 1} \tag{5.20}$$

is the spinodal in present units.

According to the general connection between the dynamical stability and the stability with respect to $\hat{T}$, the loss of dynamical stability at $K_s^{(n)}$ should be accompanied by a change in the stability character of the corresponding n-cycle. Indeed, the $n = 3$ and $n = 4$ cycles are ellitic fixed points of $\hat{T}^n$ above $K_s^{(n)}$ and transform into the hyperbolic ones at $K_s^{(n)}$.

For the modulated density configurations with larger periods the stability condition cannot be given such a simple form as (5.19). It appears, however, that the region of local stability for these states in general will be restricted to the metastable part of the phase diagram, i.e., the part between the phase coexistence curve and the spinodal. This leads to the low-temperature "phase" diagram shown in Fig. 2.

5.4. A Related Hamiltonian System

Most of the structure of the discrete map (5.6) described so far is also found in the phase portrait of a two-dimensional, Hamiltonian dynamical

system, which can be derived from the equilibrium model (4.6). Since the current $J_j(\mathbf{\rho})$ in this case is explicitly given in the form (4.4) with some ositive Onsager coefficient L_j, the condition of zero current may be replaced by the much simpler stationary condition (4.5). Together with the free energy functional (4.7) this yields

$$\rho_{j+1} - 2\rho_j + \rho_{j-1} = \frac{1}{4\beta J} \ln \frac{\rho_j}{1-\rho_j} - 4\rho_j + \tilde{\mu} \tag{5.21}$$

where the "chemical potential" $\tilde{\mu}$ controls the mean density ρ of the system; $\rho = \frac{1}{2}$ corresponds to $\tilde{\mu} = 2$. The recursion relation (5.21) defines a two-dimensional discrete dynamical system on the phase space $[0, 1]^2$ with volume-preserving dynamics. It has been studied in great detail by Pandit and Wortis.[28] We want to think of the mapping (5.21) as arising from the full three-diensional system (4.8) with $(d/dt)\,\rho_j(t) = 0$ through the appropriate restriction of the phase space which explicitly takes into account the conservation law. The third dimension would thus enter in (5.21) through the parameter $\tilde{\mu}$. Although we do not know how to perform this restriction for (5.6), the hase portrait of (5.21) will still be useful as an illustration to some features of our model. In the following, we give a brief descrition of the phase portrait. We consider the case $\rho = \frac{1}{2}$ ($\tilde{\mu} = 2$) only.

Instead of a line of fixed points, the map (5.21) has a single hyperbolic fixed point above T_c. At the critical temperature $\beta_c J = \frac{1}{4}$, it bifurcates into one elliptic and two additional hyperbolic fixed points, which correspond to the thermodynamically stable phases of high and low density, respectively. Below T_c, the elliptic fixed point emits n-cycles of arbitrarily high periods n. These appear at characteristic temperatures $T^{(n)}$, which can be obtained from the eigenvalues of the elliptic fixed point by (5.15). As above, we find $T^{(2)} = 0$. At $\beta J = \frac{1}{2}$ an elliptic 4-cycle analogous to (5.12) appears. Its density is given by

$$2\rho - 1 = \tanh\{2\beta J(2\rho - 1)\} \tag{5.22}$$

When this line in the ρ–T diagram intersects the spinodal

$$(2\rho_s - 1)^2 = 1 - \frac{1}{4\beta J} \tag{5.23}$$

approximately at $\beta J = 0.68$, the 4-cycle changes into the hyperbolic kind. A phase portrait containing the ellitic 4-cycle is shown in Fig. 3c.

In the phase portrait of (5.21) the kink solution corresponds to a trajectory connecting the unstable manifold of one hyperbolic fixed point with the stable manifold of the other. Close to T_c, when the correlation length is

large compared to the lattice spacing ($\xi \gg 1$), the discrete dynamical system (5.21) is well approximated by its continuous counterpart

$$\frac{d^2\rho}{dx^2} = \frac{1}{4\beta J} \ln\left(\frac{\rho(x)}{1-\rho(x)}\right) - 4\rho(x) + \tilde{\mu} \tag{5.24}$$

This system is integrable, and the unstable manifold of one hyperbolic fixed point coincides with the stable manifold of the other.[16] Thus the phase portrait of (5.21) close to T_c is that of a slightly perturbed integrable Hamiltonian system (Fig. 3a). Most of the phase space between the hyperbolic fixed points is filled with smooth ellitic orbits (KAM trajectories) which are stable against small perturbations. As the temperature is lowered and the discrete character of the dynamical system (5.21) becomes dominant ($\xi = 1$), more and more of the KAM trajectories are destroyed. The hyperbolic fixed points are now embedded in a growing region of unstable, chaotic trajectories which separates them from the elliptic orbits (Fig. 3b). Finally at $T = T^{(2)} = 0$ the elliptic fixed point turns hyperbolic with reflection ($\lambda_+ = \lambda_- = -1$) and no ellitic orbits remain.

5.5. Kink Solution

As already promised, our second topic is the construction of the kink solution. This is done numerically. As initial condition for the iteration of (5.6) we choose $(\beta^{-1}, \alpha^{-1}, \alpha, \beta)$ with the four points related through (5.5). Such an interface position is expected to yield an optimal kink profile.[18] The initial condition is characterized by a single parameter δ, which determines the interfacial steepness. For a fixed temperature $T < T_c$ we then perform subsequent iterations with increasing δ. When δ is small, the trajectories oscillate with a given period. The period of oscillation increases with δ. At a certain critical value δ_c the iteration leaves the physical domain. Just below δ_c, however, we generate in this way configurations where the density remains practically constant over up to several hundred lattice spacings which presumably represents a close approximation to the true kink solution.

As listed in Table II the maximal densities of these kinklike configurations lie on the phase coexistence curve of Sec. 4 for $(K_c - K)/K_c \leqslant 10^{-1}$. At lower temperatures there are deviations, and the method seems to fall completely for $(K_c - K)/K_c \geqslant 0.5$. The reason for this is most clearly illustrated by the phase portrait of the two-dimensional dynamical system (5.21) (Fig. 3). In the vicinity of the critical point, where the mapping is nearly integrable, the kink trajectory may be approximated by numerically stable KAM trajectories to a very high accuracy (Fig. 3a).

At lower temperatures the kink trajectory is embedded in a chaotic region and therefore quite impossible to locate numerically (Fig. 3b). In the context of the two-dimensional mapping our method consists of scanning the phase space with initial conditions chosen along the line $\{x+y=1\}$. Since we start at the elliptic fixed point ($\delta=0$) and move outward, the procedure terminates at the last KAM trajectory it encounters ($\delta=\delta_c$) and therefore never reaches the hyperbolic fixed points. Unlike the two-dimensional case, the full three-dimensional mapping (5.6) offers no possibility to determine the asymptotic densities of the kink without locating the corresponding trajectory. We expect nevertheless that the agreement between the kink solution and the phase coexistence curve holds also at low temperatures.

The width of the kink profile diverges as $(K_c-K)/K_c)^{-1/2}$ for $K\to K_c$, as can be seen from the last column of Table III. This is identical to the behavior of the tanh profile (4.20) arising from the continuum Cahn–Hilliard theory.

5.6. Approximate Freidlin–Wentzell-Theory

Finally we investigate the approximate low-temperature dynamics, $K<K_c=3+\sqrt{2}$, of an 8-column system with periodic boundary conditions for large N. The density is fixed at $\frac{1}{2}$. There are two stable configurations, one with period 8, denoted by $\boldsymbol{\rho}_1$, corresponding to the kink, and one with period 4, denoted by $\boldsymbol{\rho}_2$. It turns out to be useful to include also the three unstable stationary configurations. These are of period 8 ($\boldsymbol{\rho}_3$), of period 4 ($\boldsymbol{\rho}_4$), and homogeneous ($\boldsymbol{\rho}_5$). The period 4 configurations exist only for $K<K^{(4)}=3$, and $\boldsymbol{\rho}_2$ becomes stable at $K=2.4$ [cf. (5.19)].

The "quasi-potential" V_{ij} of (5.1) is the solution of the variational problem

$$V_{ij}=\inf\left\{\int_0^T S(\phi(t),\dot{\phi}(t))\,dt \,|\, \phi(0)=\boldsymbol{\rho}_i,\ \phi(T)=\boldsymbol{\rho}_j,\ T\right\} \tag{5.25}$$

$i,j=1,\ldots,5$. The action S is computable from the master equation (2.7).[26] The variation is over all paths starting at $\boldsymbol{\rho}_i$ and ending at $\boldsymbol{\rho}_j$ after an *arbitrary* passage time T. V_{ij} is computed under drastic simplifications.[22] For the action only the first and the second jump moments and not the full jump distribution are used. The paths are taken to be straight lines. Since unstable stationary configurations, i.e., saddle points are included, we hope this to be not too bad an approximation. The only variational parameter left is the passage time from $\boldsymbol{\rho}_i$ to $\boldsymbol{\rho}_j$. From this approximate V_{ij} we determine the stationary weights of $\boldsymbol{\rho}_1,\ldots,\boldsymbol{\rho}_5$ as the stationary solution of the master equation with rates (5.1).

We plot in Fig. 4 the "free energies" $f(l)$ of (5.2), obtained by this procedure, as a function of temperature. We choose the normalization $f(1)=0$. As expected, the kink solution ρ_1 carries most of the statistical weight. At low temperatures entropy effects should be small. Therefore we compare the free energies with the energies $\beta(U(\rho_i)-U(\rho_1))$, where U is computed as the average of H in (2.1). Remarkably enough, there is good qualitative agreement between energies and free energies.

Since the qualitative picture is rather insensitive to the details of the calculational procedure, we believe it to be generally correct in spite of the drastic approximations involved. Thus we conclude that the periodically modulated states obtained as cycles of the discrete dynamics (5.6) are merely metastable in the thermodynamic sense. As in equilibrium, the globally stable low-temperature state of the system is given by the kink profile.

ACKNOWLEDGMENT

We thank H. van Beijeren for very useful discussions. Part of this work was carried out while three of us, J. K., J. L. L., and H. S., were at the IHES, Bures-sur-Yvette, in the fall of 1984. This work was supported in part by NSF Grant No. DMR81-14726-03.

REFERENCES

1. S. Katz, J. L. Lebowitz, and H. Spohn, *Phys. Rev. B* **28**:1655 (1983).
2. S. Katz, J. L. Lebowitz, and H. Spohn, *J. Stat. Phys.* **34**:497 (1984).
3. A. Onuki and K. Kawasaki, *Ann. Phys. (N.Y.)* **121**:456 (1979).
4. A. Onuki, K. Yamazaki, and K. Kawasaki, *Ann. Phys. (N.Y.)* **131**:217 (1981).
5. W. Dietrich, P. Fulde, and I. Peschel, *Adv. Phys.* **29**:527 (1980), and references therein.
6. J. Marro, J. L. Lebowitz, H. Spohn, and M. H. Kalos, *J. Stat. Phys.* **38**:725 (1985).
7. J. L. Vallés and J. Marro, *J. Stat. Phys.* **43**:441 (1986).
8. J. Marro, handwritten notes.
9. H. van Beijeren and L. S. Schulman, *Phys. Rev. Lett.* **53**:806 (1984).
10. P. C. Hohenberg and B. I. Halperin, *Rev. Mod. Phys.* **49**:435 (1977).
11. K. Gadwedski and A. Kupiainen, preprint.
12. K. Leung and J. Cardy, preprint.
13. B. Schmittmann and H. K. Janssen, preprint.
14. H. van Beijeren, R. Kutner and H. Spohn, *Phys. Rev. Lett.* **54**:2026 (1985).
15. D. Forster, D. R. Nelson, and M. J. Stephen, *Phys. Rev. A* **16**:732 (1977).
16. D. A. Huse, C. L. Henley, and D. S. Fisher, *Phys. Rev. Lett.* **55**:2924 (1985).
17. M. H. Jensen and P. Bak, *Phys. Rev. B* **27**:6853 (1983).
18. R. Pandit and M. Wortis, *Phys. Rev. B* **25**:3226 (1982).
19. R. Liowsky, Thesis, LMU München, 1982.
20. T. Janssen and J. A. Tjon, *J. Phys. A* **16**:673 (1983).

21. P. I. Belobrov, V. V. Beloshapkin, G. M. Zaslavskii, and A. G. Tret'yakov, *Sov. Phys. JETP* **60**(1):180 (1984).
22. N. G. van Kampen, *Stochastic Processes in Physics and Chemistry* (North-Holland, Amsterdam, 1981).
23. T. G. Kurtz, *J. Appl. Prob.* **7**:49 (1970); **8**:344 (1971).
24. J. Krug, Diplomarbet, LMU München, 1985.
25. J. W. Cahn and J. E. Hilliard, *J. Chem. Phys.* **28**:258 (1958).
26. M. I. Freidlin and A. D. Wentzell, *Random Perturbation of Dynamical Systems* (Springer, Berlin, 1984).